

5. CONCLUSION

In this letter, as a new design method of a filter, a closed form equation of tapped feeding has been presented and discussed. Also, a $\lambda_g/2$ stub BPF and $\lambda_g/4$ stub BPF with narrow bandwidth have been presented using the equivalent circuits of the tapped-line geometry. The parameters of the tapped-line geometry are obtained by input (output) admittance toward source (load) of the filter prototype, and the proposed tapped-line geometry is composed of the open-stub and the additional transmission-line which have a negative electrical length.

The proposed design method using the equivalent circuit of the tapped-line geometry can be applied to several filters' design such as an edge-coupled filter, a combline filter, an interdigital filter, and so on. Because stub filter doesn't need coupling mechanism, its design procedures are simple. Also, the suggested stub filter design allows narrower bandwidth implementation compared to the conventional stub filter which is typically provided only with wide bandwidth. The proposed filter is easily implemented and integrated with other devices and circuits.

ACKNOWLEDGMENTS

This research has been conducted by the Research Grant of Kwangwoon University in 2008.

REFERENCES

1. E.G. Cristal, Tapped-line coupled transmission lines with applications to interdigital and combline filters, *IEEE Trans Microwave Theory Tech* 23 (1975), 1007–1012.
2. C. Ernst and V. Postoyalko, Tapped-line interdigital filter equivalent circuits, *IEEE MTT-S Symp Dig*, Denver, CO (1997), 801–804.
3. S. Caspi and J. Adelman, Design of combline and interdigital filters with tapped-line input, *IEEE Trans Microwave Theory Tech* 36 (1988), 759–763.
4. J.S. Wong, Microstrip tapped-line filter design, *IEEE Trans Microwave Theory Tech* 27 (1979), 44–50.
5. K.W. Kim, C.H. Park, and S.J. Han, A new design procedure of tapped-line filters, *Int Symp Antennas Propagat*, Monterey, CA (2004), 2863–2866.
6. J.S. Hong and M.J. Lancaster, *Microwave filters for RF/microwave applications*, Wiley, New York, 2001.
7. M.G. Lee, T.S. Yun, H. Nam, D.H. Shin, T.J. Baek, J.K. Rhee, and J.C. Lee, Millimeter-wave GaAs surface micromachined bandpass filters using the external quality factor, *J Appl Phys* 45 (2006), 6014–6016.
8. T.S. Yun, T.U. Hong, B. Lee, J.J. Choi, J.Y. Kim, K.B. Kim, and J.C. Lee, A new band-pass filter design with tapped-line using J/K-inverter, *Microwave Opt Tech Lett* 49 (2007), 1253–1256.
9. G. Matthaei, L. Young, and E.M.T. Jones, *Microwave filters, impedance-matching networks, and coupling structures*, Artech House, Norwood, MA, 1980.
10. Zeland Software. IE3D simulator, Jan. 1997.

© 2009 Wiley Periodicals, Inc.

STUDY OF A UNIPLANAR PRINTED INTERNAL WWAN LAPTOP COMPUTER ANTENNA INCLUDING USER'S HAND EFFECTS

Cheng-Tse Lee and Kin-Lu Wong

Department of Electrical Engineering, National Sun Yat-Sen University, Kaohsiung 80424, Taiwan; Corresponding author: sheng@mail.xjtu.edu.cn

Received 17 December 2007

ABSTRACT: A uniplanar monopole antenna to be printed on a thin (0.4 mm) and small-size FR4 substrate and capable of GSM850/900/1800/1900/UMTS penta-band WWAN operation for thin-profile laptop computer application is presented. The antenna is formed by a direct-fed shorter radiating strip for upper-band operation at about 1900 MHz and a coupled-fed longer radiating strip which is also short-circuited to the antenna ground for lower-band operation at about 900 MHz. Note that the two radiating strips are fed using different excitation mechanisms. With the coupling excitation and short-circuiting, which functions as an internal printed matching circuitry, the longer radiating strip can provide a wide dual-resonant lower band at around 900 MHz for GSM850/900 operation. A wide upper band can also be generated at about 1900 MHz for the antenna to cover GSM1800/1900/UMTS operation. The antenna is studied in the article, and the user's hand effects on the performances of the antenna are analyzed. The obtained results are useful for the antenna employed in the laptop computer with a touch panel. © 2009 Wiley Periodicals, Inc. *Microwave Opt Technol Lett* 51: 2341–2346, 2009; Published online in Wiley InterScience (www.interscience.wiley.com). DOI 10.1002/mop.24614

Key words: internal laptop computer antenna; printed antennas; WWAN antenna; multiband operation; user's hand effects

1. INTRODUCTION

To provide ubiquitous wireless internet access for the mobile users, the WWAN (wireless wide area network) operation in the GSM850/900/1800/1900/UMTS (824–894/890–960/1710–1880/1850–1990/1920–2170 MHz) bands has been proposed to be added and incorporated with the WLAN (wireless local area network) operation [1–9] in the modern laptop computers. For this perspective application, some possible WWAN antennas have been reported in the published articles [10–15]. The reported WWAN antennas in [10, 11] are to be embedded in the USB (universal series bus) dongle for the laptop computer and are not to be embedded inside the casing of the laptop computer as internal antennas. For the reported WWAN antennas in [12–14], they are suitable to be applied as internal antennas in the laptop computer; however, they generally show a three-dimensional structure and hence are not very promising for application in the thin-profile laptop computer, which recently attracts much attention for the mobile users. It is also noted that the reported antennas in [10–14] provide limited operating bandwidths and cannot cover all the five operating bands for WWAN operation.

Very recently, a uniplanar PIFA (planar inverted-F antenna) covering GSM850/900/1800/1900/UMTS operation in the laptop computer has been reported [15]. The PIFA is formed by two shorted radiating strips and fed by a coupling feed, and the metal pattern of the PIFA can be printed on a 0.8-mm thick substrate. In this study, a uniplanar WWAN laptop computer antenna formed by a direct-fed radiating strip for upper-band operation at about 1900 MHz and a coupled-fed short-circuited radiating strip for lower-band operation at about 900 MHz is presented. The studied antenna here uses the hybrid combination of a simple direct-fed

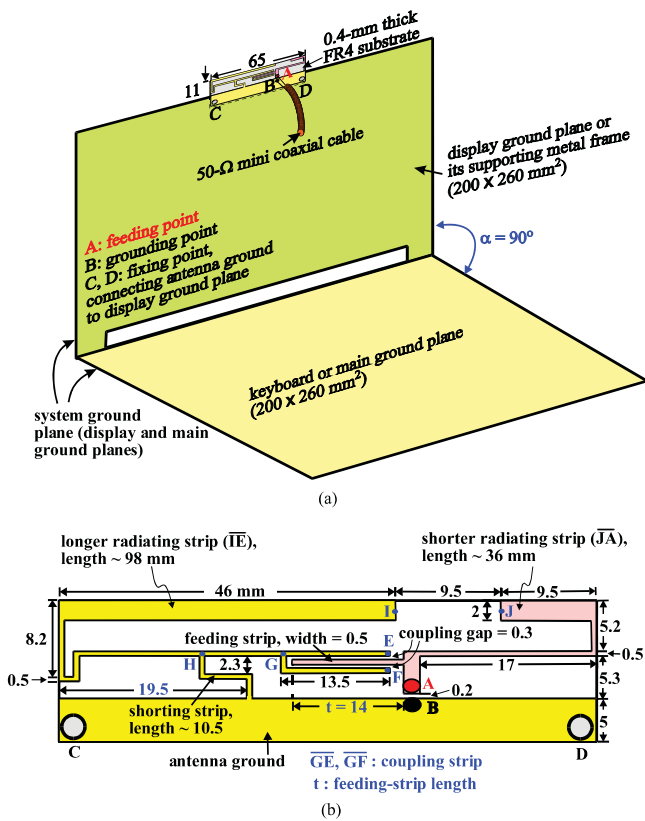


Figure 1 (a) Geometry of the studied internal uniplanar printed WWAN laptop computer antenna. (b) Detailed dimensions of the antenna's metal pattern. [Color figure can be viewed in the online issue, which is available at www.interscience.wiley.com]

monopole element and a coupled-fed shorted monopole element, different from the design in [15] and also capable of generating two wide operating bands covering GSM850/900/1800/1900/UMTS for penta-band WWAN operation. In addition, the antenna studied in this article is printed on a 0.4-mm thick FR4 substrate, thinner than that in [15], making it more attractive for thin-profile laptop computer applications. Further, a more realistic system ground plane consisting of the display ground plane (or the supporting metal frame of the laptop display) and the keyboard ground plane (or the main ground plane) is used in the study, which can provide more informative results for the internal WWAN antenna employed in the laptop computers.

For considering the case of the laptop computer equipped with a touch panel, the user's hand effects are also analyzed, because the user's hand can be very close to the embedded internal WWAN antenna, when it is pointing close to or at the top edge of the touch panel. In this case, since the user's hand is a very glossy material [16–20], its effects on the antenna performances, especially on the radiation pattern and radiation efficiency, may not be negligible. The obtained results based on the user's hand model provided by SPEAG SEMCAD [21] are presented and discussed.

2. STUDIED ANTENNA

Figure 1(a) shows the geometry of the studied uniplanar printed WWAN laptop computer antenna. Detailed dimensions of the antenna's metal pattern are given in Figure 1(b). The studied antenna is printed on one surface of a 0.4-mm thick FR4 substrate. The antenna comprises a shorter radiating strip, a longer radiating portion and an antenna ground. For application in the laptop

computer, the antenna is mounted along and at the center of the top edge of the display ground plane. Through the fixing points C and D in the antenna ground, the antenna is electrically connected to the display ground plane, which is further connected to the keyboard or main ground plane to be considered as the system ground plane in this study. Both the display and keyboard ground planes are of the same dimensions 200 × 260 mm², which are reasonable for general laptop computers. The two ground planes are fabricated using a 0.2-mm thick copper plate in the experiment, and the angle between the two ground planes are denoted as α , which is set to be 90° in the experiment.

In the studied antenna, the shorter radiating strip [section JA in Fig. 1(b)] is a simple direct-fed monopole of length about 36 mm, close to a quarter-wavelength at about 1900 MHz. One end of the shorter radiating strip is the feeding point A, which is spaced 0.2 mm to the antenna ground. Across the 0.2-mm spacing, a 50-Ω mini coaxial line is applied with its central conductor and outer grounding sheath connected to point A and point B (the grounding point in the antenna ground), respectively, for testing the antenna.

The longer radiating portion consists of a longer radiating strip (section IE) short-circuited to the antenna ground and a coupling part. The longer radiating strip has a length of about 98 mm (about a quarter-wavelength at 900 MHz) and is capacitively excited through the coupling part which comprises two coupling strips (sections GE and GF) and a feeding strip of length (t) 14 mm. The coupling excitation mechanism is applied to achieve a dual-resonance excitation in the 900 MHz band to obtain a wide operating band covering GSM850/900 operation [15, 22–25]. Also note that to enhance the coupling in the condition of a thin (0.4 mm only) dielectric substrate used, there are two coupling strips applied, both spaced a coupling gap of 0.3 mm to achieve the required coupling effect. Through adjusting the length t of the feeding strip (the length of the two coupling strips fixed to be 13.5 mm), the desired coupling effect can be controlled.

3. RESULTS AND DISCUSSION

The antenna was fabricated and tested. Figure 2 shows the measured and simulated return loss of the fabricated prototype. Good agreement between the measured data and the simulated results obtained using Ansoft HFSS [26] is verified. Two wide operating bands at about 900 and 1900 MHz are seen to be generated. With the 3:1 VSWR or 6-dB return loss definition, the bandwidths of the

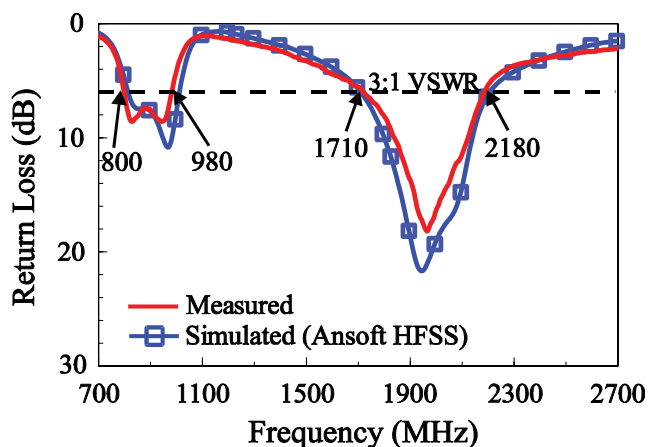
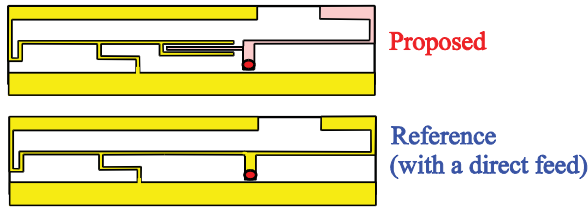
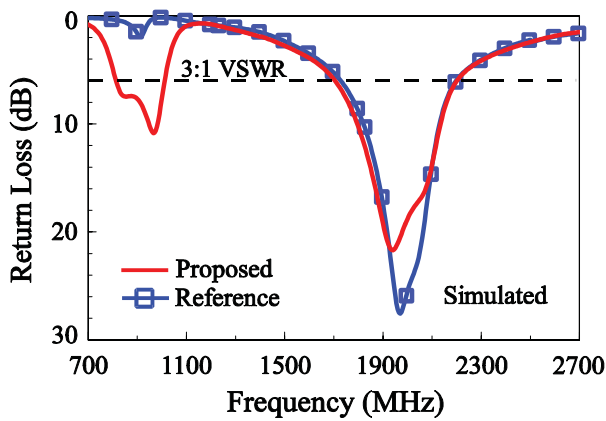
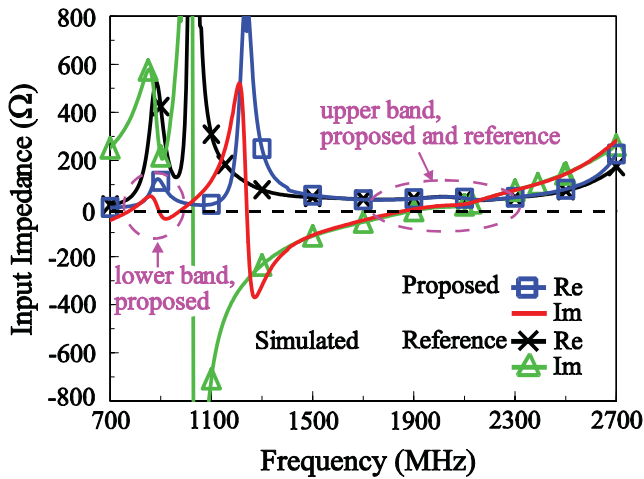


Figure 2 Measured and simulated (HFSS) return loss of the studied antenna. [Color figure can be viewed in the online issue, which is available at www.interscience.wiley.com]



(a)



(b)

Figure 3 Comparison of the HFSS simulated (a) return loss and (b) input impedance of the studied antenna and the reference antenna (corresponding PIFA with a direct feed). [Color figure can be viewed in the online issue, which is available at www.interscience.wiley.com]

two operating bands easily cover GSM850/900/1800/1900/UMTS operation.

Figure 3 shows a comparison of the simulated return loss and input impedance of the studied antenna and the reference antenna (a corresponding PIFA with a direct feed). Both the two antennas are of the same size. From the simulated return loss shown in Figure 3(a), it is observed that the lower operating band at about 900 MHz cannot be excited with good impedance matching for the reference antenna. For the upper operating band, there are very small differences for the two antennas. This can be explained from the simulated input impedance shown in Figure 3(b); it is seen that the very high input impedance level for the reference antenna at around 900 MHz is greatly decreased to be about or smaller than 100 Ω with two resonances (zero reactance), which results in the

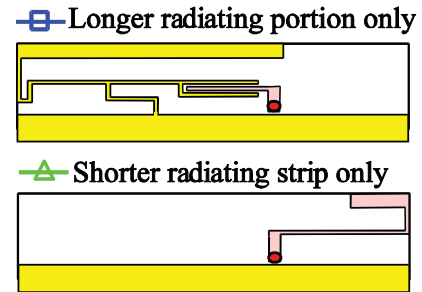
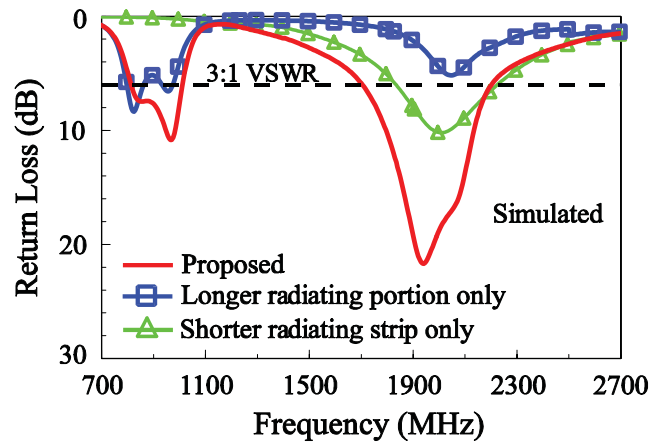


Figure 4 Simulated (HFSS) return loss of the studied antenna and the two cases with the longer radiating portion or the shorter radiating strip only. [Color figure can be viewed in the online issue, which is available at www.interscience.wiley.com]

successful excitation of a dual-resonance excitation for the desired lower operating band to cover GSM850/900 operation. As for the input impedance level at around 1900 MHz, very small differences are seen, which agrees with the results observed in Figure 3(a).

Effects of the longer radiating portion and the shorter radiating strip are studied in Figure 4. The results indicate that for the case with the shorter radiating strip only, the 900 MHz band cannot be excited and there is one resonant mode occurred at about 1900 MHz for the upper-band operation. As for the case with the longer radiating portion, the desired lower-band operation can be ob-

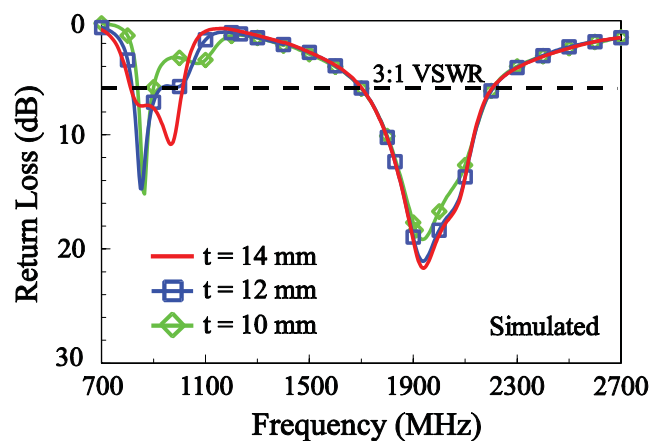


Figure 5 Simulated (HFSS) return loss as a function of the length t of the feeding strip; other dimensions are the same as given in Figure 1. [Color figure can be viewed in the online issue, which is available at www.interscience.wiley.com]

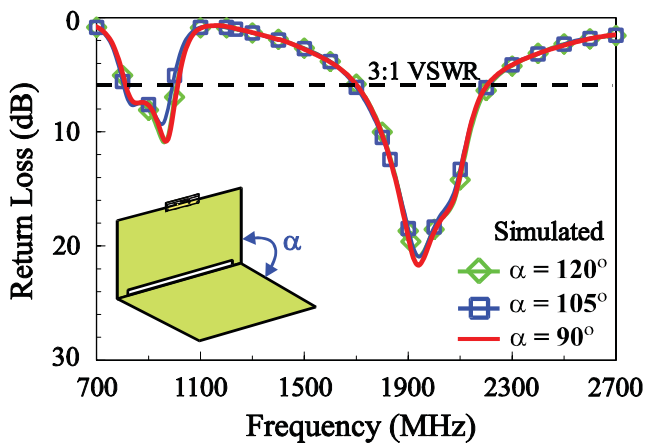


Figure 6 Simulated (HFSS) return loss as a function of the angle α between the display and main ground planes. Other dimensions are the same as given in Figure 1. [Color figure can be viewed in the online issue, which is available at www.interscience.wiley.com]

tained, and in addition, a higher-order resonant mode is excited at about 2000 MHz. This higher-order resonant mode at about 2000 MHz and the resonant mode at about 1900 MHz contributed by the shorter radiating strip are formed into the desired wide operating band for GSM1800/1900/UMTS operation.

Effects of the length t of the feeding strip are analyzed in Figure 5. The simulated return-loss results for the length t varied from 10 to 14 mm are presented. Large effects on the impedance matching of the 900 MHz band are seen. This behavior is reasonable, since the variations in the length of the feeding strip will result in variations in the capacitive excitation of the longer radiating portion. However, this also indicates that by adjusting the length t , good excitation of the desired dual-resonant lower operating band can be fine-tuned. It is also noted that very small effects are seen on the upper operating band. This behavior indicates that the desired lower and upper bands can be separately controlled by the longer radiating portion and the shorter radiating strip, respectively.

Figure 6 shows the simulated return loss as a function of the angle α between the display and main ground planes. Results show that there are very small variations for the angle α varied from 90° to 120° . This indicates that the orientation between the display and main ground planes has small effects on the impedance matching of the embedded internal WWAN antenna studied here.

Radiation characteristics of the antenna are also studied. Figure 7 plots the simulated and measured three-dimensional (3-D) total-

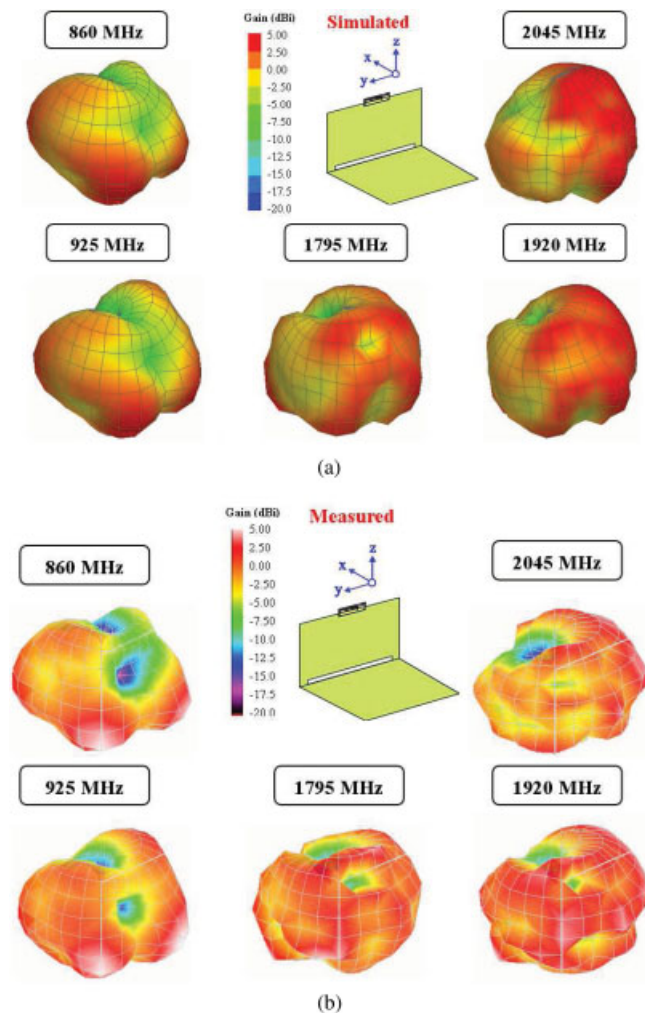


Figure 7 (a) Simulated (HFSS) and (b) measured 3-D total-power radiation patterns of the studied antenna. [Color figure can be viewed in the online issue, which is available at www.interscience.wiley.com]

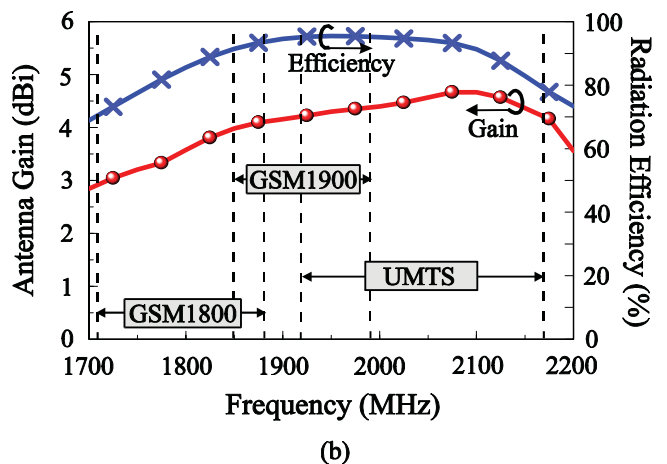
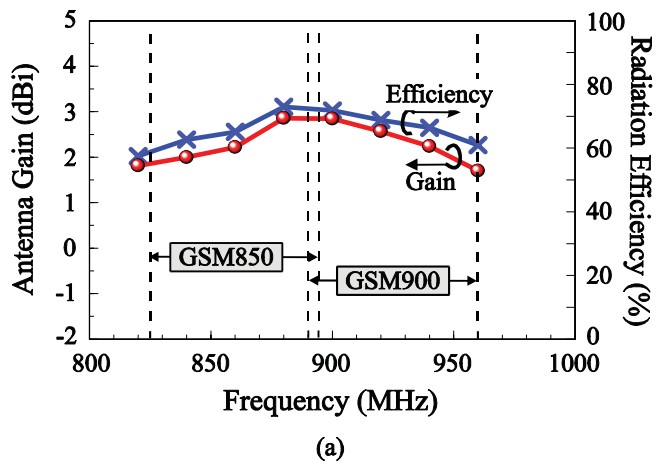


Figure 8 Measured antenna gain and radiation efficiency of the studied antenna. (a) Lower band for GSM850/900 operation. (b) Upper band for GSM1800/1900/UMTS operation. [Color figure can be viewed in the online issue, which is available at www.interscience.wiley.com]

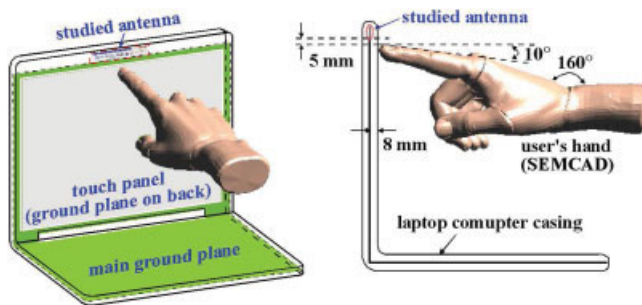


Figure 9 Simulation (SEMCAD) model of the studied antenna with the user's hand pointing at the top edge of the touch panel. [Color figure can be viewed in the online issue, which is available at www.interscience.wiley.com]

power radiation patterns of the antenna at 860, 925, 1795, 1920, and 2045 MHz, about the central frequencies of the five operating bands. The measured and simulated radiation patterns are generally seen to be in agreement. Figure 8 shows the measured antenna gain and radiation efficiency of the antenna. Over the lower band for GSM850/900 operation [Fig. 8(a)], the antenna gain is about 1.7–2.8 dBi, and the radiation efficiency is ranged from about 60–74%. Over the upper band for GSM1800/1900/UMTS operation [Fig. 8(b)], the antenna gain is about 2.9–4.7 dBi, whereas the radiation efficiency is all better than 70%.

To analyze the user's hand effects on the studied antenna, the simulation model using SEMCAD [21] shown in Figure 9 is applied. The user's hand is pointing at the top edge of the touch panel and is assumed to space 8 mm to the display ground plane and 5 mm below the antenna as shown in the simulation model. The simulated (SEMCAD) return loss for the studied antenna with and without the user's hand is shown in Figure 10. It is interesting to see that there are very small variations between the two cases of with and without the user's hand. That is, the user's hand shows very small effects on the impedance matching of the studied antenna embedded inside the laptop computer casing. However, as seen from the 3-D total-power radiation patterns at 925 and 1795 MHz for the studied antenna shown in Figure 11, large variations in the radiation patterns owing to the presence of the user's hand are seen. In addition, the radiation efficiency is decreased by about 10% at the two frequencies, when the user's hand is present. This efficiency decrease is mainly owing to the user's hand being a very lossy material [16–20] for the antenna.

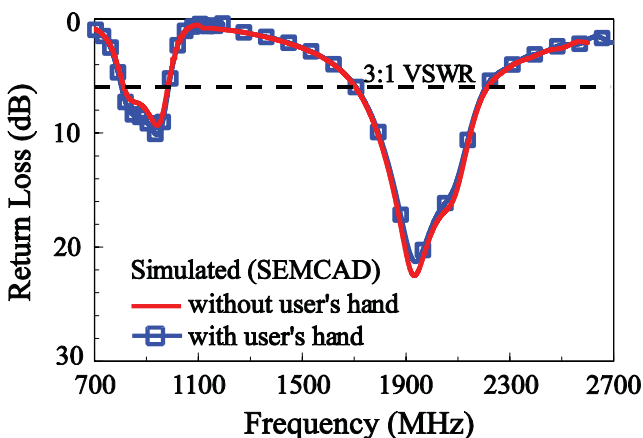
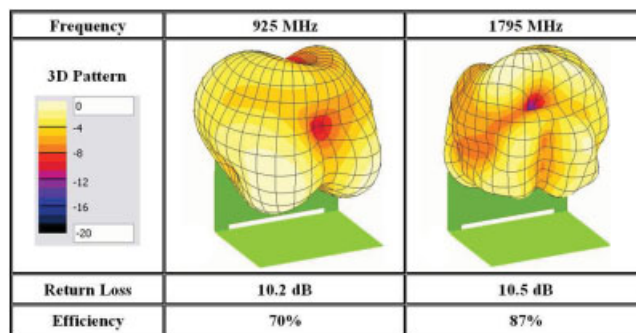
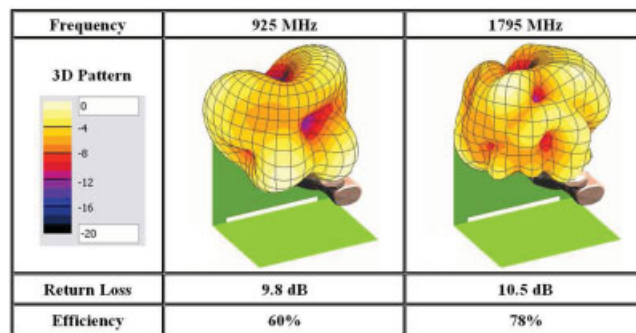


Figure 10 Simulated (SEMCAD) return loss for the studied antenna with and without the user's hand. [Color figure can be viewed in the online issue, which is available at www.interscience.wiley.com]



(a)



(b)

Figure 11 Simulated (SEMCAD) 3-D total-power radiation patterns at 925 and 1795 MHz for the studied antenna. (a) Without the user's hand. (b) With the user's hand. [Color figure can be viewed in the online issue, which is available at www.interscience.wiley.com]

4. CONCLUSION

A uniplanar printed monopole antenna easy to fabricate on a very thin (0.4 mm) FR4 substrate at low cost for GSM850/900/1800/1900/UMTS operation in the modern thin-profile laptop computer has been proposed. The antenna is formed by a simple direct-fed monopole element and a coupled-fed shorted monopole element. Two wide operating bands at about 900 and 1900 MHz have been obtained for the desired penta-band operation. In addition, the capacitive coupling mechanism between the two monopole elements in the studied antenna allows the two generated wide bands to be adjusted separately, which makes the antenna easy to fine-tune in practical applications. For the case of the laptop computer with a touch panel, the user's hand effects have also been analyzed. Results have shown that there are large effects on the radiation pattern and radiation efficiency of the antenna embedded inside the laptop computer, owing to the presence of the user's hand in the vicinity of the antenna. This behaviour is similar to the user's hand effects observed for the internal mobile phone antennas [16–20].

REFERENCES

1. D. Liu and B. Gaucher, A triband antenna for WLAN applications, IEEE Antennas Propagat Soc Int Symp Dig 2, Columbus, OH, 2003, pp. 18–21.
2. Y.L. Kuo and K.L. Wong, Printed double-T monopole antenna for 2.4/5.2 GHz dual-band WLAN operations, IEEE Trans Antennas Propagat 51 (2003), 2187–2192.
3. T. Hosoe and K. Ito, Dual-band planar inverted F antenna for laptop computers, IEEE Antennas Propagat Soc Int Symp Dig 3, Columbus, OH, 2003, pp. 87–90.
4. C.M. Su, W.S. Chen, Y.T. Cheng, and K.L. Wong, Shorted T-shaped

monopole antenna for 2.4/5 GHz WLAN operation, *Microwave Opt Technol Lett* 41 (2004), 202–203.

5. J. Yeo, Y.J. Lee, and R. Mittra, A novel dual-band WLAN antenna for notebook platforms, *IEEE Antennas Propagat Soc Int Symp Dig*, Monterey, CA, 2004, pp. 1439–1442.
6. K.L. Wong, L.C. Chou, and C.M. Su, Dual-band flat-plate antenna with a shorted parasitic element for laptop applications, *IEEE Trans Antennas Propagat* 53 (2005), 539–544.
7. L. Lu and J.C. Coetzee, A modified dual-band microstrip monopole antenna, *Microwave Opt Technol Lett* 48 (2006), 1401–1403.
8. L.C. Chou and K.L. Wong, Uni-planar dual-band monopole antenna for 2.4/5 GHz WLAN operation in the laptop computer, *IEEE Trans Antennas Propagat* 55 (2007), 3739–3741.
9. K.L. Wong, *Planar antennas for wireless communications*, Chapter 5, Wiley, New York, 2003.
10. K.L. Wong and C.H. Kuo, Internal GSM/DCS/PCS antenna for USB dongle application, *Microwave Opt Technol Lett* 48 (2006), 2408–2412.
11. W.C. Su and K.L. Wong, Internal PIFAs for UMTS/WLAN/WiMAX multi-network operation for a USB dongle, *Microwave Opt Technol Lett* 48 (2006), 2249–2253.
12. C.H. Kuo, K.L. Wong, and F.S. Chang, Internal GSM/DCS dual-band open-loop antenna for laptop application, *Microwave Opt Technol Lett* 49 (2007), 680–684.
13. X. Wang, W. Chen, and Z. Feng, Multiband antenna with parasitic branches for laptop applications, *Electron Lett* 43 (2007), 1012–1013.
14. K.L. Wong and L.C. Chou, Internal cellular/WLAN combo antenna for laptop-computer applications, *Microwave Opt Technol Lett* 47 (2005), 402–406.
15. K.L. Wong and S.J. Liao, Uniplanar coupled-fed printed PIFA for WWAN operation in the laptop computer, *Microwave Opt Technol Lett* 51 (2009), 549–554.
16. C.M. Su, C.H. Wu, K.L. Wong, S.H. Yeh, and C.L. Tang, User's hand effects on EMC internal GSM/DCS dual-band mobile phone antenna, *Microwave Opt Technol Lett* 48 (2006), 1563–1569.
17. C.I. Lin and K.L. Wong, Printed monopole slot antenna for internal multiband mobile phone antenna, *IEEE Trans Antennas Propagat* 55 (2007), 3690–3697.
18. C.I. Lin and K.L. Wong, Internal meandered loop antenna for GSM/DCS/PCS multiband operation in a mobile phone with the user's hand, *Microwave Opt Technol Lett* 49 (2007), 759–765.
19. W.Y. Li, K.L. Wong, and J.S. Row, Study of the planar DTV antenna in the portable media player held by the user's hands, *Microwave Opt Technol Lett* 49 (2007), 1841–1844.
20. C.H. Wu and K.L. Wong, Internal shorted planar monopole antenna embedded with a resonant spiral slot for penta-band mobile phone application, *Microwave Opt Technol Lett* 50 (2008), 529–536.
21. Available at: <http://www.semcad.com>, SPEAG SEMCAD, Schmid & Partner Engineering AG.
22. K.L. Wong and C.H. Huang, Bandwidth-enhanced PIFA with a coupling feed for quad-band operation in the mobile phone, *Microwave Opt Technol Lett* 50 (2008), 683–687.
23. C.H. Chang, K.L. Wong and J.S. Row, Coupled-fed small-size PIFA for penta-band folder-type mobile phone application, *Microwave Opt Technol Lett* 51 (2009), 18–23.
24. C.H. Chang and K.L. Wong, Internal coupled-fed shorted monopole antenna for GSM850/900/1800/1900/UMTS operation in the laptop computer, *IEEE Trans Antennas Propagat* 56 (2008), 3600–3604.
25. K.L. Wong and C.H. Huang, Printed PIFA with a coplanar coupling feed for penta-band operation in the mobile phone, *Microwave Opt Technol Lett* 50 (2008), 3181–3186.
26. Available at: <http://www.ansoft.com/products/hf/hfss/>, Ansoft Corporation HFSS, Pittsburgh, PA.

© 2009 Wiley Periodicals, Inc.

MICROSTRIP BANDPASS FILTER DESIGN USING TRIANGULAR OPEN LOOP RESONATORS WITH IMPROVED CROSS-COUPLED STRUCTURE

Haiwen Liu and Mingtao Tan

School of Information Engineering, East China Jiaolong University, Shuanggang Road, Changbei, Nanchang 330013, China; Corresponding author: liuhaiwen@gmail.com

Received 2 January 2009

ABSTRACT: In this letter, a highly selective microstrip bandpass filter using triangular open-loop resonators with improved cross-coupled structure is designed, fabricated, and measured. The new cross coupling structure is implemented by inserting two L-shaped stubs into the triangular open-loop resonators. A good agreement is achieved between simulated and measured results. Measurements are given to verify that a passband from 5.1 to 5.5 GHz with the insertion loss less than 1.0 dB and return loss more than 20 dB is obtained. There are two transmission zeros on both sides of the passband which lead to higher selectivity for the passband. In addition, two extra transmission zeros are observed obviously and located at about 7.0 GHz and 9.0 GHz, respectively, for high out-of-band rejection. The filter has a compact size of 10 mm × 6 mm which amounts to about 0.3 λ_g × 0.2 λ_g . © 2009 Wiley Periodicals, Inc. *Microwave Opt Technol Lett* 51: 2346–2348, 2009; Published online in Wiley InterScience (www.interscience.wiley.com). DOI 10.1002/mop.24599

Key words: bandpass filter; cross coupling, triangular open loop resonator; transmission zeros; microstrip circuit

1. INTRODUCTION

Rapid development of wireless communications and radar technology presents extraordinary demands for microstrip open-loop resonator filters with low insertion loss, high selectivity and high out-of-band rejection [1, 2]. In general, half-wavelength open loop resonators and more than two resonator units are adopted popularly. Furthermore, folded type resonators such as stepped-impedance resonator (SIR) and hairpin resonator are applied widely to reduce the circuit size [3, 4]. In those filter designs, novel cross coupling technologies, i.e., multilayer cross-coupled resonator, defected SIR, are usually used to improve the skirt slope and enhance the selectivity [5, 6]. However, multilayer structure and defected ground circuit improve the circuit cost and design complexity.

Recently, much attention has been paid to the cascaded quadruplet (CQ) filters, and the nonadjacent coupling is used to realize transmission zeros on each side of the passband symmetrically by several groups [7, 8]. For example, Liao proposed a method of double cross-coupling lines to produce the transmission zeros independently in the both close-to-band rejections of high temperature superconductor (HTS) filter to achieve the improved skirt slope. And Wu used nonresonating nodes to generate N transmission zeros out of N resonators without directly coupling the source to the load and reduce the sensitivity of the filters to manufacturing errors [9, 10].

In this letter, we present a highly selective microstrip bandpass filter that consists of only two triangular open-loop resonators loaded two L-shaped stubs. Cross-coupling structure is implemented by inserting these two L-shaped stubs into the triangular open-loop resonators. Simulated and measured are given to prove that the proposed filter is compact and exhibits excellent filtering performances.